Highlights of 2020

Welcome

Professor Kouichi Ono
Editor-in-Chief

Welcome to the Highlights of 2020 collection for *Applied Physics Express* (APEX) and the *Japanese Journal of Applied Physics* (JJAP). We are pleased to present this collection of articles specially selected by the Editorial team to highlight the scientific quality of research published in the journals last year.

APEX and JJAP are the flagship journals of the Japan Society of Applied Physics. Both are international journals with authors from across Asia-Pacific, North America, Europe and the Middle East, and read by researchers from 4,000 organisations worldwide, both in scientific/academic institutions as well as researchers working in industry R&D. APEX and JJAP publish scientific work that significantly contributes to the advancement of technological innovation. Over 5,000 articles from both APEX and JJAP have been referenced in more than 26,000 patents.

During 2020, we have seen fantastic engagement from the international community of applied physics online, with over 400 instances of APEX and JJAP research being discussed or mentioned in social media, news sites and science blogs.

In this collection, we present a sample of the excellent research published in the journals during 2020. Articles in this collection were selected by the Editors as particularly noteworthy, reflecting a diversity of topics and authors in APEX and JJAP.

We are extremely proud of the quality and speed of our peer review service, offering authors rapid decision times of just 13 days from submission to first decision after peer review for APEX, and 27 days for JJAP. The journals also offer our authors a high impact channel to publish their research. In 2020, APEX's Impact Factor increased to 3.086, its highest Impact Factor to-date, while JJAP's Impact Factor remained stable at 1.376. This reflects the continued support of the international applied physics community to both our journals.

Finally, on behalf of the Editorial Boards of APEX and JJAP, I would like to thank all our authors and reviewers for the invaluable contribution that they have made to the success of the journals.

Electrical properties and conduction mechanisms of heavily B^+-ion-implanted type IIa diamond: effects of temperatures during the ion implantation and postannealing upon electrical conduction

Yuhei Seki *et al* 2020 *Jpn. J. Appl. Phys.* **59** 021003

✚ Open abstract View article PDF

We investigated the electrical properties and conduction mechanism of heavily B+-implanted type IIa diamond with respect to the implantation and postannealing temperatures. The B atoms were shallowly implanted with a flat concentration of 3.5 × 1019 cm^{-3} at RT and 900°C; these samples were finally annealed at 1150°C, 1300°C and 1450°C. We consequently confirmed p-type conductivity and typical ionization energy of acceptor B in a wide measured temperature range. The doping efficiency attained 78% and the Hall mobility at RT was realized to be 108 $cm^2V^{-1}s^{-1}$ for the RT-implanted sample followed by annealing at 1300°C. On the other hand, hot B+-implantation at 900°C slightly degraded the electrical properties. The higher-temperature annealing at 1450°C after B^+-implantation promoted hopping conduction fairly well at a lower measured temperature range below around RT. We systematically investigated the hopping conduction mechanism based on theoretical relations.

Coulomb-limited mobility in 4H-SiC MOS inversion layer as a function of inversion-carrier average distance from MOS interface

Munetaka Noguchi *et al* 2020 *Jpn. J. Appl. Phys.* **59** 051006

✚ Open abstract View article PDF

In Si-face 4H-SiC metal-oxide-semiconductor field-effect transistors (MOSFETs) with nitrided gate oxide, inversion layer mobility decreases at higher acceptor concentrations. This is attributed to rapid decrease in Coulomb-limited mobility ($\mu_{Coulomb}$). However, the causes for this decrease have not been fully understood yet. In this study, $\mu_{Coulomb}$ is experimentally determined using samples with various acceptor concentrations by varying the body bias. To well formulate $\mu_{Coulomb}$, the depletion-charge and surface-carrier densities in the inversion layer are found to be important parameters. Furthermore, to deepen the physical understanding, $\mu_{Coulomb}$ is investigated from the viewpoint of the inversion-carrier average distance from the MOS interface (ZAV). It is established that ZAV can universally describe $\mu_{Coulomb}$ in the inversion layer of Si-face 4H-SiC MOSFETs with nitrided gate oxide.

Effect of chemical interaction at modification layer/substrate interface on molecular orientation of dinaphtho[2,3-*b*:2',3'-

f]thieno[3,2-*b*]thiophene thin films

Kazuaki Iwasawa and Koji K. Okudaira 2020 *Jpn. J. Appl. Phys.* **59** 091004

✚ Open abstract View article PDF

Towards the sophisticated process integration, we discuss the molecular orientation and the electronic structure of dinaphtho[2,3-b:2',3'-f]thieno[3,2-b]thiophene (DNTT) thin films on modified substrates, which are treated by self-assembling molecules with multifunctional moieties. DNTT thin films on modified silicon dioxide (SiO_2) and copper oxide (CuO_x) substrates whose surfaces were treated by 6-[(3-trisilanol)propylamino]-1,3,5-triazine-2,4-bis(2-aminoethylamine) (TAS) were investigated using near-edge X-ray absorption fine structure and ultraviolet/X-ray photoelectron spectroscopy. The interfacial dipole by the chemical interaction at the TAS/substrate interface can stabilize the standing orientation of DNTT molecules on TAS-modified SiO_2 and CuO_x surfaces. An opposite TAS orientation due to different reaction sites in TAS provided a stronger interfacial dipole at the TAS/CuO_x interface by 0.3 eV compared with the TAS/SiO_2 interface. In addition, the terminal functional groups at the outermost surface of TAS caused the difference in the intermolecular distance of the DNTT thin films.

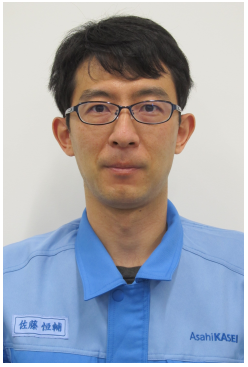

Room-temperature operation of AlGaN ultraviolet-B laser diode at 298 nm on lattice-relaxed $Al_{0.6}Ga_{0.4}N$/AlN/sapphire

Kosuke Sato *et al* 2020 *Appl. Phys. Express* **13** 031004

✚ Open abstract View article PDF

In this paper, AlGaN ultraviolet-B laser diode at 298 nm on a sapphire substrate was realized operated at room temperature under pulse conditions by applying two key technologies; a growing method of lattice-relaxed n-$Al_{0.6}Ga_{0.4}N$ layers and a design of composition-graded p-AlGaN cladding layers. The n-$Al_{0.6}Ga_{0.4}N$ with the threading dislocation density of 1×10^9 cm^{-2} was grown on a sputtered and annealed AlN/sapphire at first with three-dimensional island shapes followed by a two-dimensional film overgrowth to confine most of the dislocations within the islands. The durable composition-graded p-AlGaN was developed with a first graded undoped AlGaN (320 nm) with Al compositions linearly changing from 0.9 to 0.45 and a second graded Mg-doped AlGaN (75 nm) with Al compositions from 0.45 to 0. AlGaN UV LDs will be developed using this structure as a fundamental design in future works.

OPEN ACCESS

Room-temperature continuous-wave operation of green vertical-cavity surface-emitting lasers with a curved mirror fabricated on {20−21} semi-polar GaN

Tatsushi Hamaguchi *et al* 2020 *Appl. Phys. Express* **13** 041002

✚ Open abstract View article PDF

We demonstrate a room-temperature continuous-wave operation of green vertical-cavity surface-emitting laser (VCSEL) with a 20 μm long cavity possessing a dielectric curved mirror formed over a {20-21} semi-polar gallium nitride substrate. The emission wavelength and the threshold current were 515 nm and 1.8 mA, respectively. We also confirmed that white light is generated by overlaying three prime colors of light, i.e. red, blue and green, emitted only from VCSEL. The cavity of the proposed VCSEL consists of ridge waveguides formed by RIE connecting two dielectric DBRs formed by vacuum deposition on the edges. We believe all those could be introduced to other material systems than nitrides to enable wider practical uses of VCSELs across ultraviolet to infra-red deeper than ever.

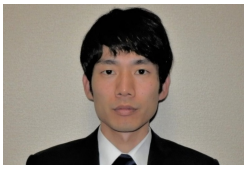

Room-temperature continuous-wave operations of GaN-based vertical-cavity surface-emitting lasers with buried GaInN tunnel junctions

Kazuki Kiyohara *et al* 2020 *Appl. Phys. Express* **13** 111003

✚ Open abstract View article PDF

We have successfully demonstrated the room-temperature (RT) continuous-wave (CW) operations of GaN-based vertical-cavity surface-emitting lasers with buried GaInN tunnel junctions (BTJ-VCSELs). We first estimated an influence of an absorption loss at the GaInN TJ on laser performance by using one-dimensional transmission matrix method. The simulation results predicted a 5.5λ-cavity GaInN BTJ-VCSEL can reduce internal loss by 2.5 cm^{-1} compared to a 4λ-cavity VCSEL with an ITO intracavity contact. Then, we have achieved RT CW operations of the GaInN BTJ-VCSELs, showing a low operating voltage of 5.3 V at 10 kA cm^{-2} and a differential resistance of 110 Ω for the 8 μm aperture case. The maximum output power reached 2.0 mW for the VCSEL with the 10 μm diameter aperture.

OPEN ACCESS

Record high extraction efficiency of free electron laser oscillator

Heishun Zen *et al* 2020 *Appl. Phys. Express* **13** 102007

✚ Open abstract View article PDF

The highest extraction efficiency (9.4%) of a free electron laser (FEL) oscillator has been achieved at the midinfrared FEL facility of Kyoto University. Because of the interaction between the electron beam and FEL electromagnetic field, a maximum electron energy decrease of 16% was observed. The measured energy decrease

was consistent with the measured FEL spectrum. An FEL micropulse energy of ~100 μJ with the expected few-cycle pulse duration at a wavelength of 11 μm was observed. In this condition, the intracavity micropulse energy (8.3 mJ) was expected to exceed the total kinetic energy of the electron bunch (5.4 mJ). This result is an important milestone for the high-extraction-efficiency FEL oscillator and will contribute to the strong-field physics of atoms and molecules.

Nano-height cylindrical waveguide in GaN-based vertical-cavity surface-emitting lasers

Masaru Kuramoto *et al* 2020 *Appl. Phys. Express* **13** 082005

✚ Open abstract View article PDF

We have proposed a novel nano-height cylindrical waveguide in blue GaN-based vertical-cavity surface-emitting lasers (VCSELs). The proposed 5 nm step height cylindrical waveguide using simple processes provides lateral optical confinement and excellent performance in terms of light output power and wall plug efficiency (WPE). A fabricated multi-mode VCSEL with 7 mu;m emission diameter achieved a light output power of 23.7 mW, maximum external differential quantum efficiency of 43.6%, and WPE of 10% under continuous wave operation at 20 °C. Additionally, a single-mode blue VCSEL with a 3.3-μm emission diameter and a 5-nm step height cylindrical waveguide achieved a wall plug efficiency of 9.9% and a light output power of 5 mW. These findings indicate that VCSEL devices are very sensitive to nanostructure changes among semiconductor laser diodes. Hence, future studies on not only nano-epitaxial technology, but also the nano-fabrication process, will empower future GaN-based VCSELs and expand their range of applications.

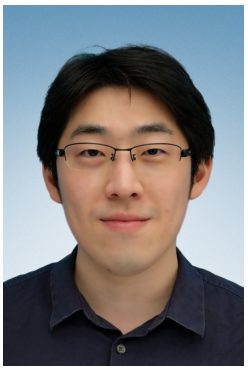

Heat flux sensing by anomalous Nernst effect in Fe–Al thin films on a flexible substrate

Weinan Zhou and Yuya Sakuraba 2020 *Appl. Phys. Express* **13** 043001

✚ Open abstract View article PDF

The transverse electric field generated by the anomalous Nernst effect (ANE) in a magnetic material allows different design principles for thermoelectric generation devices, and is receiving increased attention from the viewpoints of fundamental physics and practical applications. Here, we discussed the potential of using the ANE for heat flux sensing, and performed a numerical analysis of the material parameters required for such an application. Then, we experimentally studied the ANE of epitaxial Fe-Al thin films and found a large anomalous Nernst thermopower S_{ANE} = 3.4 μV K^{-1} in $Fe_{81}Al_{19}$. Using this material, we fabricated a prototype ANE-based heat flux sensor on a thin flexible polyimide sheet and

demonstrated accurate sensing with it. This study shows that a simple-structured, flexible, and low-thermal-resistance heat flux sensor can be realized by exploiting the ANE, and presents important information for further enhancing its sensitivity.

Guiding of dynamic skyrmions using chiral magnetic domain wall

Moojune Song *et al* 2020 *Appl. Phys. Express* **13** 063002

✚ Open abstract View article PDF

Magnetic skyrmions are in the spotlight as a novel information carrier for emerging magnetic devices because of their extremely small size and high speed. However, when the skyrmion moves along a nanotrack, its trajectory is curved due to the skyrmion Hall effect, leading to a collision and an annihilation of the skyrmion at the physical edge. This is detrimental in terms of data preservation, but hard to avoid in real devices. We propose a method to prevent edge-induced skyrmion annihilation by using a chiral magnetic domain wall as a boundary. Using micromagnetic simulations, we found that the stability of the skyrmion is increased several times by replacing the conventional edge with a domain wall boundary. We also provide device architectures that enable the guiding, sorting and size-tuning of multiple skyrmions, which could be potentially useful for future skyrmion devices.

Magnetic tunnel junctions with metastable bcc Co_3Mn electrodes

Kazuma Kunimatsu *et al* 2020 *Appl. Phys. Express* **13** 083007

✚ Open abstract View article PDF

Magnetic tunnel junctions (MTJs), exhibiting tunnel magnetoresistance (TMR) effect, is a key device for spintronics and are utilized for commercial hard disk reading heads, magnetoresistive random access memories (MRAM), and magnetic sensors. In this paper, Kunimastu et al. reported MTJs comprising unconventional bcc type Co-Mn alloy electrodes. Co-Mn alloys have fcc and hcp crystalline structures as thermodynamically stable phases and show ferri- or anti-ferromagnetism; thus unsuitable for MTJs. Kunimatsu et al. obtained metastable bcc type Co-Mn alloy films, and they discovered the large TMR effect greater than 200 (600) % at room (low) temperature. This finding would accelerate to explore advanced materials for MTJs and contribute to develop MTJs-based advanced applications, such as high density MRAM, high-frequency devices, and unconventional computing.

OPEN ACCESS

Two-dimensional multicolor (RGBY) integrated nanocolumn micro-LEDs as a fundamental technology of micro-LED display

Katsumi Kishino *et al* 2020 *Appl. Phys. Express* **13** 014003

✚ Open abstract View article PDF

The development of high-productivity micro light-emitting diode (μ-LED) pixel panels is crucial as a key technology for next-generation displays. To provide a fundamental approach to this end, the monolithic integration of multicolor nanocolumn (NC) μ-LED pixels with 5 × 5 μm^2 emission windows arranged at intervals of 10-μm was demonstrated for fabricating multicolor integrated μ-LED pixel units. These integrated units were two-dimensionally arranged in an 8 × 8 square lattice, and the individual μ-LED pixels were independently driven, exhibiting a μ-LED pixel panel arrangement. The color of the emissions for InGaN/GaN ordered NC arrays changed with increasing NC diameter (D). For one multicolor integrated unit comprising four ordered NC arrays with different values of D, the blue, green, yellow, and red emissions were observed to exhibit electroluminescence spectra with peak wavelengths of 478, 512, 559, and 647 nm, respectively.

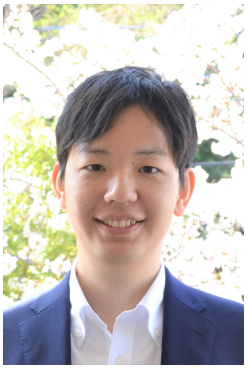

Liquid helium-free high-T_c superconducting terahertz emission system and its applications

Yoshihiko Saiwai *et al* 2020 *Jpn. J. Appl. Phys.* **59** 105004

✚ Open abstract View article PDF

We constructed a compact THz emission-detection system based upon the emitters developed by us from the intrinsic Josephson junctions in single crystals of high-T_c superconducting $Bi_2Sr_2CaCu_2O_{8+\delta}$ cooled by a Stirling cryocooler and detected with a Schottky barrier diode detector operated at room temperature. The output from the THz emitter operated by the Stirling cooler is applied to a three-dimensional (3D) THz computer tomography imaging. This compact emission-detection system may be regarded as a prototype of commercial THz wave systems based upon high-T_c superconducting devices, and allows us to make an easy to use compact 3D THz imaging system providing for the next stage of THz applications.

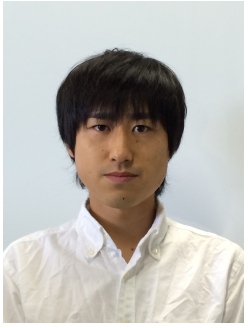

Fabrication of folded bilayer-bilayer graphene/hexagonal boron nitride superlattices

Takuya Iwasaki *et al* 2020 *Appl. Phys. Express* **13** 035003

✚ Open abstract View article PDF

Carbon-based superlattices represent a novel class of quantum metamaterials having promising prospects. Here we show the first fabrication of folded bilayer-bilayer graphene (fBBLG)/hexagonal boron nitride (hBN) superlattices. In the transport properties

at low temperatures, satellite peaks are observed due to the crystallographic angle alignment of fBBLG and hBN. The peculiar resistance peaks appear away from the charge neutrality point and the hBN-induced satellites, which may be signatures of possible competing orders. Our results suggest the emergence of a unique electronic band-structure in the fBBLG, providing a way for investigating the correlated electron phenomena by performing energy-band engineering with superlattice structures.

The optimization of surface plasmon coupling efficiency in InGaN/GaN nanowire based nanolasers

Di Jiang *et al* 2020 *Appl. Phys. Express* **13** 085001

✚ Open abstract View article PDF

Since 2003, Stockman and Bergman proposed the concept, and Zhang et al. experimentally demonstrated the surface plasmon laser, which aroused widespread concern in academia. Our group have been concentrated on the research of low threshold GaN-based plasmon nanolaser in 2017. In this study, we systematically optimized the surface plasmon coupling efficiency with different structural parameters. The threshold of plasmon nanolaser with cavity sizes beyond optical diffraction limit has reached as low as ~4 W/cm^2 and the Q factor up to 196, which may convert the original cognition of laser. Such low threshold nanolaser with ultrafast laser modulation and extremely small cavity size may pave the way for the development of high efficiency nanolaser for various applications, including biochemical sensing, super-resolution imaging, and optical communication in the future.

OPEN ACCESS

Reduction in dislocation densities in 4H-SiC bulk crystal grown at high growth rate by high-temperature gas-source method

Norihiro Hoshino *et al* 2020 *Appl. Phys. Express* **13** 095502

✚ Open abstract View article PDF

We performed fast crystal growth of 4H-SiC using a high-temperature gas-source method at a growth temperature of 2550 °C and investigated the grown crystal to reveal changes in dislocation densities along the growth direction. The remarkable reduction in densities of threading and basal plane dislocations to be less than 1/10 and 1/20, respectively, was confirmed in a crystal grown at ~3 mm/h by successive grinding and performing synchrotron X-ray topography. The change in the radial distribution of threading dislocations indicates enhanced reduction in the dislocation densities in an area containing high density dislocations. We discussed possible mechanisms which could explain the declining densities of threading

dislocations along the growth direction according to the results obtained by classifying threading dislocations into each Burgers vector and investigating number of reduced dislocations in each growth stage for different areas.

Temperature dependence of internal quantum efficiency of radiation for the near-band-edge emission of GaN crystals quantified by omnidirectional photoluminescence spectroscopy

Kazunobu Kojima *et al* 2020 *Appl. Phys. Express* **13** 105504

✚ Open abstract View article PDF

The technical development of highly efficient electronic and optical devices based on semiconductor crystals is necessary toward the realization of energy-saving society. In this article, a method to detect light-emitting efficiency of the semiconductor crystals was proposed by optical probing technique named omnidirectional photoluminescence (ODPL) spectroscopy. The ODPL method is an ideal method to quantify the internal quantum efficiency (IQE) of radiation for condensed-matter placed outside an integrating sphere, and is applicable to large size crystals or semiconductor wafers. The method realizes the efficiency detection under very low temperature (-261 °C) and can find the point defects and nonradiative impurities even with a dilute concentration.

Reduction of plasma-induced damage in n-type GaN by multistep-bias etching in inductively coupled plasma reactive ion etching

Shinji Yamada *et al* 2020 *Appl. Phys. Express* **13** 016505

✚ Open abstract View article PDF

Plasma-induced damage in n-type GaN was reduced by multistep-bias etching that involved a stepwise decrease of the etching bias power (P_{bias}) in inductively coupled plasma reactive ion etching (ICP-RIE) and subsequent annealing. The depth of damage at P_{bias} = 60 W, which has a high etching rate, was determined to be 60 nm from the capacitance-voltage characteristics of Ni/Al_2O_3/etched-GaN metal-oxide-semiconductor diodes. The damaged layer was removed by subsequent lower bias power etching at P_{bias} = 5 W and 2.5 W. The residual and shallow damage induced by the low P_{bias} was then recovered by subsequent annealing at 400 °C. The multistep-bias etching of ICP-RIE was thus confirmed to be effective for achieving a high etching rate with low damage.

3D impurity profiles of doped/intrinsic amorphous-silicon layers composing textured silicon heterojunction solar cells detected by atom probe tomography

Yasuo Shimizu *et al* 2020 *Appl. Phys. Express* **13** 126503

+ Open abstract View article PDF

An amorphous-Si (a-Si)/crystalline-Si (c-Si) heterojunction (SHJ) is a promising solar cell structure that enables high conversion efficiency. The very thin (< 10 nm) a-Si layers deposited on pyramidal textured c-Si surfaces are the dominant factors to determine the output performance. Atom probe tomography (APT) was utilized for elemental mapping in a-Si layers of textured SHJ solar cells. Owing to a site-specific lift-out method using focused ion beam, one can select an arbitrary pyramidal surface for APT analysis. In addition, a time-of-flight mass spectrometer equipped in APT is equally sensitive to all elements, and has the potential to detect H atoms in hydrogenated a-Si layers. This paper provides the dopant profiles in p- and n-type a-Si layers and standard guidelines for the assessment of the H content in a-Si of SHJ solar cells.

High-speed multi-beam X-ray imaging using a lens coupling detector system

Tetsuroh Shirasawa *et al* 2020 *Appl. Phys. Express* **13** 077002

+ Open abstract View article PDF

With the growing interest in dynamical phenomena in various fields of fundamental and industrial sciences, the high-speed X-ray imaging technique has significantly grown in the past two decades. For the high-speed 3D imaging of non-repeatable phenomena, generally the temporal resolution is as low as subsecond since it requires a rotation of the sample. A promising approach is the X-ray multi-beam technique, which can illuminate a sample from multiple directions simultaneously and requires no sample rotation. The authors utilized a multi-beam X-ray optics and a detector system and successfully obtained nine projection images of a sample at once with an exposure time of 0.5 ms. They captured the dynamical behaviors of a light-bulb filament and a living ladybug with a temporal resolution of 0.5 ms and a spatial resolution of 70 μm, demonstrating the potential of the high-speed and high-spatial-resolution 3D imaging.

Electronic properties and primary dissociation channels of fluoromethane compounds

Toshio Hayashi *et al* 2020 *Jpn. J. Appl. Phys.* **59** SJJE02

+ Open abstract View article PDF

We investigated fluoromethane compounds (CF_4, CF_3, CHF_3, CH_2F_2, and CH_3F) to examine their electronic properties and primary dissociation channels by using computational chemistry.

Through the examination, it was revealed that many of the observed values (ionization and appearance, electron attachment, and excitation energies) were represented precisely and clarified for the ambiguously discussed phenomena. In the case of ionization for CF_3 radical, which is ionized by a lower energy than the vertical ionization energy. This phenomenon is explained by auto ionization caused in deforming from C_{3v} (pyramidal) structure to D_{3h} (planar) one in excitation and ionization processes. In the excitation process, CHF_3 and CH_3F are affected by Jahn-Teller distortion. It is clarified by pursuing excitation process from CHF_3 to CHF_2 + F that the potential curve has a shallow potential well and therefore this dissociation does not spontaneously occur and may be caused by a perturbation such as a surface interaction.

OPEN ACCESS

Impact of defects in self-assembled monolayer on humidity sensing by molecular functionalized transistors

Takahisa Tanaka *et al* 2020 *Jpn. J. Appl. Phys.* **59** SIIE04

✚ Open abstract View article PDF

To realize highly sensitive and selective sensors, numerical study of transistors functionalized with a defected self-assembled monolayer (SAM) was performed. Adsorption of water molecules on the defected SAM was treated by molecular dynamics calculations. Based on time dependent atomic positions and charges, carrier concentration and threshold voltage of defected SAM functionalized transistors were derived from the Poisson equation. The defects of the SAM caused a penetration of water molecules. Due to a strong polarization of water molecules, the water molecules penetrating the defects were stacked in the same direction. The alignment of the water molecules in the defects generated a large electrical dipole, and the threshold voltage of the transistors were shifted. The stacking of adsorbates in defects indicated the possibility to enhance not only the sensitivity but also the selectivity of SAM functionalized transistors.

2.5D integration using inductive-coupling TSV-less miniature interposer achieving 317 Gb/s/mm^2, 1.2 pJ/b data-transfer

Kota Shiba *et al* 2020 *Jpn. J. Appl. Phys.* **59** SGGL06

✚ Open abstract View article PDF

2.5D integration is achieved using inductive coupling in place of bump connections. The size of the interposer is less than 1/34 that of conventional technology, leading to cost saving without compromising area and energy efficiency. A 40 nm CMOS test chip is fabricated and data-transfer performance of 317

Gb/s/mm^2, 1.2 pJ/b is measured. Moreover, it is shown the area and energy efficiency of this technique could be improved more than linearly in accordance with the technology scaling rules.

Low-temperature (150 °C) processed metal-semiconductor field-effect transistor with a hydrogenated In–Ga–Zn–O stacked channel

Yusaku Magari *et al* 2020 *Jpn. J. Appl. Phys.* **59** SGGJ04

✚ Open abstract View article PDF

We developed low-temperature (150 °C) processed top-gate and coplanar metal-semiconductor field-effect transistors (MES-FETs) with a stacked In–Ga–Zn–O (IGZO) channel consisting of a hydrogenated IGZO (IGZO:H) on conventional IGZO (IGZO). The IGZO and IGZO:H were prepared by Ar+O2 and Ar+O2+H2 sputtering, respectively. In the case of conventional MES-FETs with homogeneous IGZO channel, there is a trade-off between the on-current and off-current in the transfer characteristics. By applying the stacked channel, the on-current significantly increased while maintaining a low off-current, and it exhibited the highest on-off current ratio of 4.2 × 108 among the reported IGZO-based MES-FETs. It was found that hydrogens in IGZO:H improved Schottky interface quality, while diffused hydrogens to IGZO enhanced carrier concentration in the IGZO:H/IGZO interface, which acts as a pseud two-dimensional electron gas. The proposed method successfully demonstrated great potential for future flexible electronics applications.

JOURNAL LINKS

Submit an article

About the journal

Editorial Board

Author guidelines

Publication charges

News and editorial

Awards

Journal collections

Pricing and ordering

Contact us

Japanese Journal of Applied Physics